Journal of Physics: Conference Series **688** (2016) 012053 doi:10.1088/1742-6596/688/1/012053

Numerical Modeling of Complex Targets for High-Energy-Density Experiments with Ion Beams and other Drivers

Alice Koniges[1,a], Wangyi Liu[1], Steven Lidia[1], Thomas Schenkel[1], John Barnard[2], Alex Friedman[2], David Eder[2], Aaron Fisher[2], and Nathan Masters[2]

[1] Lawrence Berkeley National Laboratory
[2] Lawrence Livermore National Laboratory

Abstract. We explore the simulation challenges and requirements for experiments planned on facilities such as the NDCX-II ion accelerator at LBNL, currently undergoing commissioning. Hydrodynamic modeling of NDCX-II experiments include certain lower temperature effects, e.g., surface tension and target fragmentation, that are not generally present in extreme high-energy laser facility experiments, where targets are completely vaporized in an extremely short period of time. Target designs proposed for NDCX-II range from metal foils of order one micron thick (thin targets) to metallic foam targets several tens of microns thick (thick targets). These high-energy-density experiments allow for the study of fracture as well as the process of bubble and droplet formation. We incorporate these physics effects into a code called ALE-AMR that uses a combination of Arbitrary Lagrangian Eulerian hydrodynamics and Adaptive Mesh Refinement. Inclusion of certain effects becomes tricky as we must deal with non-orthogonal meshes of various levels of refinement in three dimensions. A surface tension model used for droplet dynamics is implemented in ALE-AMR using curvature calculated from volume fractions. Thick foam target experiments provide information on how ion beam induced shock waves couple into kinetic energy of fluid flow. Although NDCX-II is not fully commissioned, experiments are being conducted that explore material defect production and dynamics.

1 Introduction

The Neutralized Drift Compression Experiment II (NDCX-II) is an induction accelerator. A key feature of NDCX-II is time-of-flight longitudinal "drift compression" of a section of the beam to achieve a high intensity pulse; this is a process analogous to chirped-pulse compression of a short-pulse laser beam. A head-to-tail velocity gradient is imparted to the ion beam by a set of induction cells (accelerating elements), and the pulse then compresses as it drifts down a beam line, in a neutralizing plasma environment which provides space-charge compensation. NDCX-II will accelerate a beam containing 20-70 nC of Li+ or He+ ions to 1.2-3 MeV and compress it into a sub-nanosecond pulse at the target with an 1-mm radius spot size when fully commissioned. The machine is an induction linac with custom voltage waveforms to control the longitudinal space charge forces and compress the pulse. Overall longitudinal compression factors of ˜500X are required to achieve a 1-ns pulse, but most of that compression occurs in the accelerator [1]. In order to minimize the accelerator length and to optimize the usage of pulsed power, an initial stage of non-neutral beam compression will shorten the pulse length from 500 ns to less than 70 ns by utilizing the first few induction cells after the injector. A diagram of NDCX-II is given in Fig. 1 with the details of the end station and induction cell given.

[a] e-mail: aekoniges@lbl.gov

Content from this work may be used under the terms of the Creative Commons Attribution 3.0 licence. Any further distribution of this work must maintain attribution to the author(s) and the title of the work, journal citation and DOI.
Published under licence by IOP Publishing Ltd

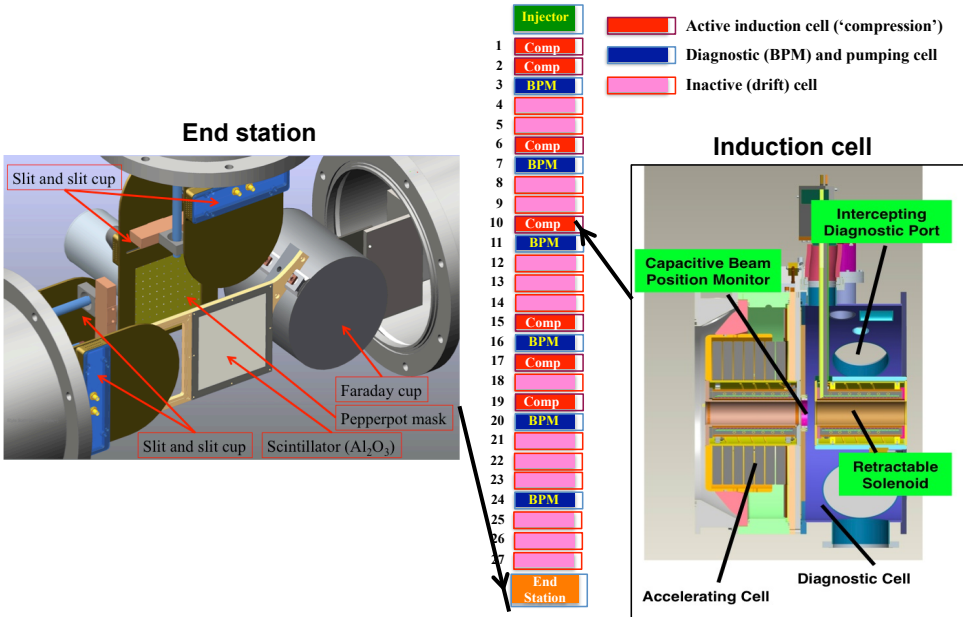

Fig. 1. NDCX-II consists of 27 induction, diagnostic, and drift cells for acceleration and pulse shaping.

2 Axisymmetric target models

When the range of the ion beam exceeds the thickness of the material being heated (thin targets), the material can be heated quite uniformly. If the timescale is sufficiently short, and the ion energy is slightly above the peak energy in dE/dX (the Bragg peak) when it enters the foil and slightly below the Bragg peak when it exits the foil the resulting temperature will be quite uniform, as the local temperature will be proportional to dE/dX. Over time a rarefaction wave propagates towards the center of the foil, and the heated material propagates rapidly outward at speeds characteristic of the sound speed. Characteristics of these rarefaction waves in ion heated metallic foils and foams can be measured via pyrometry, imaging, VISAR, and/or X-ray imaging diagnostics. By comparing the temperature, velocity, and density information obtained from these diagnostics and comparing to hydrodynamic simulations with different candidate equations of state we may distinguish between the candidate equations of state. Although the initial energy of NDCX-II will be below the Bragg peak for most materials and the hydrodynamic timescale will be somewhat shorter than the pulse duration, simulations show that approximately uniform conditions will still be created. Several experiments for NDCX-II can be modeled in 2D exploiting the axial symmetry present in the ion beam and target. Figure 2 shows 2D axisymmetric ALE AMR simulation of an expanding foil for NDCX-II parameters[2]. The simulation results of density and temperature compare well with results from a standard Inertial Fusion Energy modeling code, Hydra.

In the warm dense matter regime, the material does not expand significantly during heating, thus achieving a mostly uniform density/temperature phase. We model this state using the ALE-AMR code to solve the plasma/fluid equations given here in indicial notation ($i, j, k = 1, 2, 3$) as:

$$\frac{\mathrm{D}\rho}{\mathrm{D}t} = -\rho\nabla\cdot\mathbf{U} = -\rho U_{i,i} \tag{1}$$

$$\rho\frac{\mathrm{D}\mathbf{U}}{\mathrm{D}t} = \frac{1}{\rho}\nabla\cdot\boldsymbol{\sigma} = \frac{1}{\rho}\sigma_{ij,j} \tag{2}$$

$$\frac{\mathrm{D}e}{\mathrm{D}t} = \frac{1}{\rho}V\boldsymbol{s}:\dot{\boldsymbol{\varepsilon}} - P\dot{V} = \frac{1}{\rho}V\left(s_{ij}\dot{\varepsilon}_{ij}\right) - P\dot{V} \tag{3}$$

where $\frac{\mathrm{D}}{\mathrm{D}t} = \frac{\partial}{\partial t} + \mathbf{U}\cdot\nabla$ is the substantial derivative, ρ is the density, $\mathbf{U} = (u, v, w)$ is the material velocity, t is time, $\boldsymbol{\sigma}$ is the total stress tensor, P is the pressure, e is the internal energy, V is the relative volume

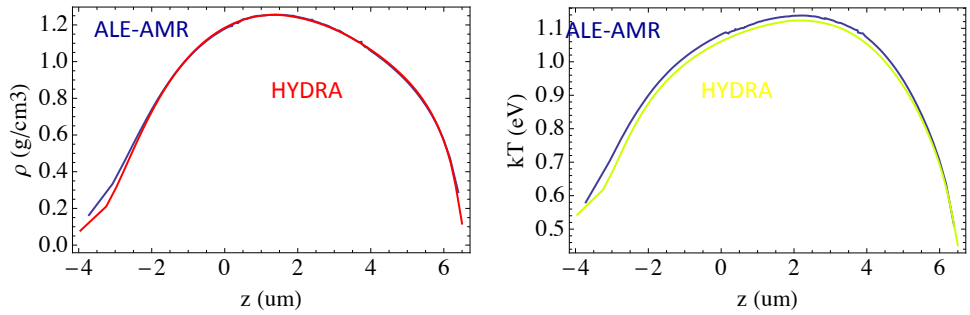

Fig. 2. Density and temperature profiles at the completion of the 1 ns, 2.8 MeV, Li ion heating pulse along the radial center of an Al foil. Fluence of 20 J/cm2.

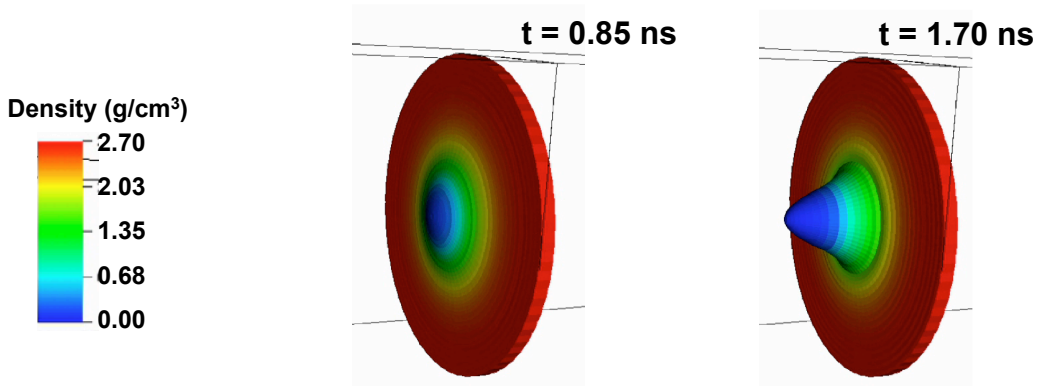

Fig. 3. ALE-AMR 2D simulation of thin foil heating experiment after the completion of the heating pulse at 0.85 ns (left) and after at 1.70 ns (right). Density contours are shown in color. The longitudinal scale is exaggerated relative to the transverse. The radius of the simulated target is 1 mm, while the thickness of the original target is 1.0 μm.

($\rho V = \rho_0$ where ρ_0 is the reference density), $\boldsymbol{s}$ is the deviatoric stress, and $\dot{\boldsymbol{\epsilon}}$ is the strain rate tensor defined as $\dot{\epsilon}_{ij} = \frac{1}{2}\left(\frac{\partial U_i}{\partial x_j} + \frac{\partial U_j}{\partial x_i}\right)$. For details see Koniges, et al.[3]. Thermal conduction is modeled using a finite element diffusion solver[4]. In Fig. 3 results of an ALE-AMR simulation confirm that there is little hydrodynamic motion during the heating phase. Note: longitudinal scale is exaggerated.

3 Droplet formation models

Some physical processes such as droplet formation and material failure are intrinsically 3D in nature. Droplets were observed in earlier NDCX-I experiments. When the target bunches up into droplets, much of the incident beam current passes through the target to be detected by the current transformer downstream of the target. Another indication of droplet formation comes from the intensity measurements where after a few microseconds, the light intensity from the target begins to decrease. One explanation for this effect is the reduction in projected surface area, as the approximately 200-nm thick foil breaks into of order 1000 nm-sized radius droplets. It is important to model this process of droplet formation and subsequent dynamics. The 3D ALE-AMR code has ion, x-ray and laser deposition, radiation hydrodynamics, thermal diffusion, anisotropic material strength with material time history, and advanced models for fragmentation including void insertion. When solid material fails in the context of a material failure condition in the code, a small volume of void is inserted in the zone. If the zone is stretched due to tensile forces or a divergent velocity field, the majority of the volume increase in the zone is due to void growth. The interface reconstruction scheme allows for void regions in neighboring zones to merge and can produce fragments of material surrounded by void[5]. We have

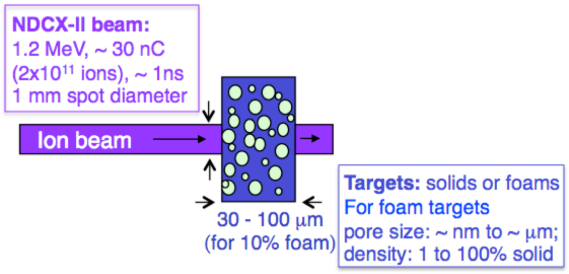

Fig. 4. Potential NDCX-II foam experimental configuration.

implemented a similar approach for modeling breakup of droplets. The full discussion of this model is being presented in a longer paper.

4 Current and future experiments

In its current state, NDCX-II can be used for lower beam power density experiments. The short excitation pulse with tunable intensity and time profile enables pump/probe type studies of defect dynamics in a broad range of materials[6]. Some capabilities of ALE-AMR including material histories and multiple levels of refinement to support different physics models at the finest scale may enable modeling of such experiments in the future. We are exploring the use of a hierarchical material model format introduced within ALE-AMR's flexible material modeling framework to study defect formation and dynamics. Additional experiments proposed for NDCX-II require full commissioning, namely full beam power and focusing capability. A potential experimental configuration is diagramed in Fig. 4. ALE-AMR is also a candidate for modeling such experiments. The experiments would be used to study warm dense matter over a range of densities by using a combination of solid and foam targets.

5 Acknowledgements

We acknowledge the National Energy Research Scientific Computing Center, supported by the Office of Science, U.S. Department of Energy under Contract No. DE-AC02-05CH11231. Work by LBNL under DE-AC02-05CH11231 was supported by the Director, Office of Science of the U.S. Department of Energy and the Petascale Initiative in Computational Science and Engineering. Work by LLNL was performed under the auspices of the U.S. Department of Energy by Lawrence Livermore National Security, LLC, Lawrence Livermore National Laboratory under Contract DE-AC52-07NA27344.

References

1. A. Friedman, J. Barnard, R. Cohen, D. Grote, S. Lund, W. Sharp, A. Faltens, E. Henestroza, J. Jung, J. Kwan et al., Phys. Plasmas **17**, 056704 (2010)
2. A.E. Koniges, N.D. Masters, A.C. Fisher, R.W. Anderson, D.C. Eder, T.B. Kaiser, D.S. Bailey, B. Gunney, P. Wang, B. Brown et al., Journal of Physics: Conference Series **244**, 032019 (2010)
3. A. Koniges, N. Masters, A. Fisher, D. Eder, W. Liu, R. Anderson, D. Benson, A. Bertozzi, Plasma Science and Technology **17**(2), 117 (2015)
4. A. Fisher, D. Bailey, T. Kaiser, D. Eder, B. Gunney, N. Masters, A. Koniges, R. Anderson, Plasma Science and Technology **17**(2), 109 (2015)
5. D. Eder, A. Fisher, A. Koniges, N. Masters, Nuclear Fusion **53**(11), 113037 (2013)
6. T. Schenkel, S. Lidia, C. Weis, W. Waldron, J. Schwartz, A.M. Minor, P. Hosemann, J. Kwan, Nuclear Instruments and Methods in Physics Research Section B: Beam Interactions with Materials and Atoms **315**, 350 (2013)